College of Engineering

Onset of Tethered Chain Overcrowding

William Y. Chen,[1] Joseph X. Zheng,[1] Stephen Z. D. Cheng,[1,*] Christopher Y. Li,[2] Ping Huang,[1] Lei Zhu,[3] Huiming Xiong,[1] Qing Ge,[1] Ya Guo,[1] Rodric P. Quirk,[1] Bernard Lotz,[4] Lingfeng Deng,[5] Chi Wu,[5] and Edwin L. Thomas[6]

[1]*Maurice Morton Institute and Department of Polymer Science, The University of Akron, Akron, Ohio 44325-3909, USA*
[2]*Department of Materials Science and Engineering, Drexel University, Philadelphia, Pennsylvania, 19104, USA*
[3]*Polymer Program, Institute of Materials Science and Department of Chemical Engineering, The University of Connecticut, Storrs, Connecticut 06269-3136, USA*
[4]*Institute of Charles Sadron, 6 Rue Boussingault, Strasbourg 67083, France*
[5]*Departments of Physics and Chemistry, Hong Kong Chinese University, Sha Tin, Hong Kong*
[6]*Department of Materials Science and Engineering, Massachusetts Institute of Technology, Cambridge, Massachusetts, 02139, USA*

(Received 3 October 2003; published 7 July 2004)

We proposed an approach to precisely control the density of tethered chains on solid substrates using PEO-*b*-PS and PLLA-*b*-PS. As the crystallization temperature T_x increased, the PEO or PLLA lamellar crystal thickness d_L increased as well as the reduced tethering density $\tilde{\sigma}$ of the PS chains. The onset of tethered PS chains overcrowding in solution occurs at $\tilde{\sigma}^* \sim 3.7$–$3.8$ as evidenced by an abrupt change in the slope between $(d_L)^{-1}$ and T_x. This results from the extra surface free energy created by the tethered chain that starts to affect the growth barrier of the crystalline blocks.

DOI: 10.1103/PhysRevLett.93.028301 PACS numbers: 83.80.Uv

In the past decade, it has been recognized that polymer brushes are key to enabling a wide range of potential surface applications related to bio- and nanotechnologies. Several approaches on how to tether chains, both neutral and charged, to substrates have been proposed [1–3]. In addition to physical absorption, chemically grafting chains onto substrates can be accomplished via "grafting to" [4] or "grafting from" polymerizations [5]. Both approaches lack the precise control needed for uniform chain tethering density (σ) and/or uniform chain length (monodisperse) of the tethered polymers.

So far, most theoretical treatments of tethered chains on flat solid substrates have been focused on the description of the noninteracting ("mushrooms") regime or the strongly stretched ("brushes") regime. It has been found that the transition between these two regimes is rather broad allowing a crossover regime to exist. The quantity σ has been frequently used to describe how close a tethered chain is to its neighbors, and it is defined by the reciprocal of the area covered by each tethered chain [6]. The reduced tethering density ($\tilde{\sigma}$) (which ignores the interaction between tethered chains and substrates) is independent of molecular weight (MW) and type of solvent used. It is defined by $\tilde{\sigma} = \sigma \pi R_g^2$, where the R_g is the radius of gyration of a tethered chain at specific experimental conditions (i.e. solvent and temperature). The physical meaning of $\tilde{\sigma}$ can be understood as how many tethered chains are in the area πR_g^2 covered by a chain in an unperturbed conformation in the same solvent [7].

As schematically shown in Fig. 1, when tethered chains are in the noninteracting regime, their tethering behavior can be approximated by renormalization group theory [8]. When the tethered chains enter the crossover regime with weak to intermediate interactions, the "single-chain mean-field theory" can be used to describe the interactions [9]. The strongly stretched regime can be treated with the numerical, self-consistent-field theory [10], Monte Carlo [11] and scaling methods [12]. However, the location of the boundaries between each of these two regimes is not quantitatively known. In experiments, most results concern the noninteracting and crossover regimes. One study showed that the strongly stretched regime was not reached at $\tilde{\sigma} \sim 12$ [7]. On the other hand, another study reported that tethered chains started to be stretched at an estimated $\tilde{\sigma} \sim 6$, but the sample

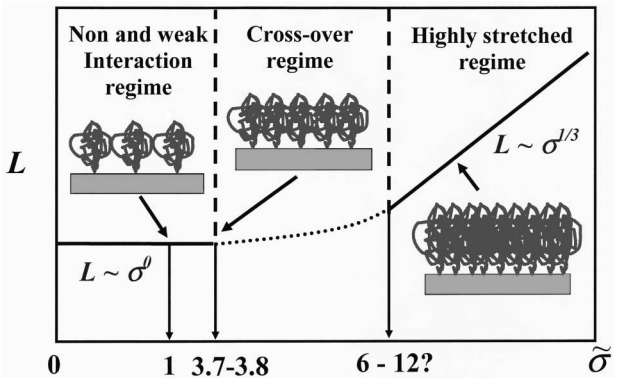

FIG. 1. Schematic representation of the thickness of tethered chains on a substrate in solution versus $\tilde{\sigma}$. The $\tilde{\sigma} = 1$ is the reference point at which tethered chains starts to laterally interact with each other. Note that the tethered chains start to get squeezed by their neighbors at $\tilde{\sigma}^* \sim 3.7$–$3.8$ (based on this work).

 0031-9007/04/93(2)/028301(4)$22.50

employed had a broad MW distribution (PDI = 1.7) [13], which likely affected the results. Therefore we asked, when do the tethered chains start to get squeezed by their neighbors? So far, theoretical predictions and experimental observations have not provided a quantitative answer to this question.

In order to answer this question, it is first necessary to precisely control the $\tilde{\sigma}$ and its local uniformity on a substrate with a near monodisperse set of tethered chains. We have developed a *crystal surface engineering* route to generate tethered chains on a single crystal basal surface using crystalline-amorphous block copolymers. In a variety of solvents, the poly(ethylene oxide) (PEO) blocks of dilute PEO-*b*-polystyrene (PEO-*b*-PS) diblock copolymer solutions and the poly(*L*-lactic acid) (PLLA) blocks in dilute PLLA-*b*-polystyrene (PLLA-*b*-PS) diblock copolymer solutions can form large sized single crystals having PS blocks covering the top and bottom of the PEO or PLLA basal surfaces to form a ''sandwiched'' layer structure [14]. The most thermodynamically stable state is a uniform distribution of the PS blocks located on both of the surfaces. Since the PEO and PLLA blocks are near monodisperse, and the number of folds for each PEO or PLLA block in the PEO or PLLA crystals is constant at a fixed crystallization temperature (T_x) in a specific solvent, so the basal surface area covered by each tethered PS chain should be identical. Furthermore, it is known that with increasing T_x, the crystalline block crystal thickness (d_L) increases (the number of folds decreases) following a relationship of $d_L \propto 1/\Delta T$ (where $\Delta T = T_d - T_x$, and T_d is the equilibrium dissolution temperature of the crystal in the solvent). Therefore, robust control of the $\tilde{\sigma}$ of the tethered PS chains on the crystal basal surface can be achieved by adjusting T_x, solvent, and/or the MWs of the blocks. In this study, two PEO-*b*-PS and two PLLA-*b*-PS diblock copolymers with different molecular weights in two different solvents (in a chrolobenzene/octane mixed solvent or in amyl acetate) are investigated.

Figure 2(a) shows a square-shaped single crystal of the PEO-*b*-PS in bright field transmission electron microscopy (TEM, JEOL 1200 EX II). The number average MW of the PEO blocks, M_n^{PEO}, was 11 kg/mol, while the M_n^{PS} was 4.6 kg/mol ($\mathrm{PDI}^{\mathrm{PS}} = 1.01$, $\mathrm{PDI}^{\mathrm{overall}} = 1.03$). The crystal was grown in the mixed solvent. The inset of Fig. 2(a) is an electron diffraction pattern of this crystal in the correct orientation. The two pairs of strongest diffraction spots were attributed to the (120) planes, indicating that the PEO chain direction in the crystal is parallel to the surface normal. The four edges of this single crystal are bounded by four (120) planes. A polyethylene (PE) decoration method [15] was also used to determine the surface orientation of the single crystal of PEO-*b*-PS. The random orientation of those rods revealed that the PE chains have, as expected, decorated the featureless amorphous PS layer surface.

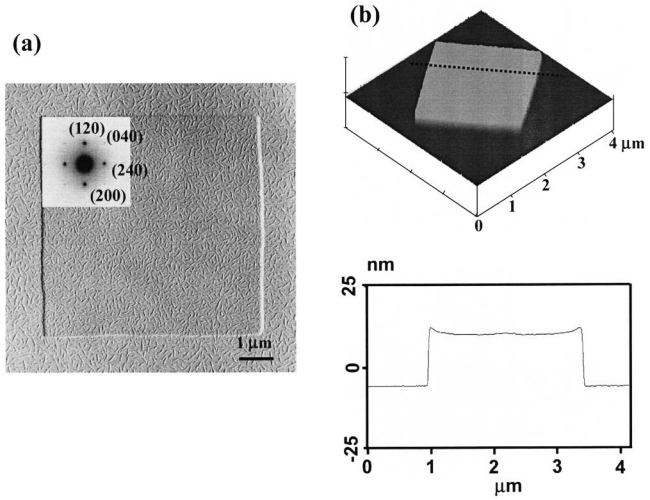

FIG. 2. TEM BF (a) image and AFM height image (b) of a square-shaped ''sandwiched'' single crystal of the PEO-*b*-PS diblock copolymer crystallized at $T_x = 25.4\,^{\circ}\mathrm{C}$ in cholorobenzene/octane dilute solution. The inset in (a) is an (hk0) SAED of this single crystal with assignments of crystallographic planes. The random PE rod crystals decorated on the surface indicate that the single crystal surface was covered by the amorphous PS blocks.

Figure 2(b) is an atomic force microscopy (AFM, DI Nanoscope IIIA) height image of the PEO-*b*-PS single crystal crystallized at 25.4 °C. The overall lamellar thickness, d_{overall}, was 15.5 nm. As a first approximation, we assumed that the density of two PS layers was identical to that of the amorphous PS bulk ($\rho_{\mathrm{PS}}^{a} = 1.052\ \mathrm{g\,cm^{-3}}$). The ρ_{PEO}^{c} and ρ_{PEO}^{a} at room temperature were also assumed identical to the bulk crystal density of 1.239 and 1.124 $\mathrm{g\,cm^{-3}}$, respectively. The PEO blocks in this system possessed 95% crystallinity ($\mathcal{W}_{\mathrm{PEO}}^{c}$) [16]. Using the equation $d_L^{\mathrm{PEO}} = d_{\mathrm{overall}} \times V_{\mathrm{PEO}}$ (%), the thickness of the PEO layer, d_L^{PEO}, could be estimated.

$$d_L^{\mathrm{PEO}} = d_{\mathrm{overall}} \times \frac{M_n^{\mathrm{PEO}}/(\mathcal{W}_{\mathrm{PEO}}^{c}\rho_{\mathrm{PEO}}^{c} + \mathcal{W}_{\mathrm{PEO}}^{a}\rho_{\mathrm{PEO}}^{a})}{M_n^{\mathrm{PEO}}/(\mathcal{W}_{\mathrm{PEO}}^{c}\rho_{\mathrm{PEO}}^{c} + \mathcal{W}_{\mathrm{PEO}}^{a}\rho_{\mathrm{PEO}}^{a}) + M_n^{\mathrm{PS}}/\rho_{\mathrm{PS}}}.$$

The d_L^{PEO} was also verified by a seeding experiment. We used the PEO-*b*-PS single crystals as seeds for further crystal growth of a homo-PEO fraction. The added homopolymer fraction can only nucleate on the (120) facets of the PEO block crystal to grow a homo-PEO single crystal. The initial thickness of the homo-PEO lamellar crystals connected with the block PEO crystal can be readily measured by AFM, and serves as direct evidence of the d_L^{PEO} in the PEO-*b*-PS single crystal. In the T_x regime studied, the observed homo-PEO initial lamellar thicknesses were identical to the d_L^{PEO} calculated from the equation. Figure 3(a) shows the relationship of the d_L^{PEO} with respect to T_x for the crystals of this PEO-*b*-PS grown in the mixed solvent. This figure also includes

data obtained in another PEO-*b*-PS diblock copolymer ($M_n^{PEO} = 40.1$ k g/mol, $M_n^{PS} = 7.7$ k g/mol, $PDI^{PS} = 1.01$, $PDI^{overall} = 1.06$) in amyl acetate dilute solution. Both of the d_L^{PEO} initially increase with T_x. After T_x reached 27.2 °C for the first sample and 28.3 °C for the second sample, the rate of d_L^{PEO} increase changed.

The PEO blocks generate a fixed number of folds (and thus, stems) in the crystal covered by two tethered PS layers at each T_x. For the first PEO-*b*-PS sample, e.g., the $T_x = 25.4$ °C while $d_{overall} = 15.5$ nm and $d_L^{PEO} = 10.5$ nm. Thus, $d^{PS} = 2.5$ nm. Using the definition of $d^{PS}\rho_{PS}N_A/M_n^{PS}$ (where N_A is the Avogadro number), we calculated that $\sigma = 0.34/nm^2$. Similar calculations were also carried out for the second PEO-*b*-PS sample.

Figure 3(b) shows two relationships between $(d_L^{PEO})^{-1}$ and T_x using the d_L^{PEO} data in Fig. 3(a). Below $T_x^* = 27.2$ °C for the first sample, the relationship was almost linear (for discussion, see below). At the T_x^*, a slope decrease appeared due to the fact that the d_L^{PEO} was only slightly increased above this T_x^*. Since the R_g of the PS chains (R_g^{PS}) of $M_n^{PS} = 4.6$ k g/mol in the mixed solvent was 1.8 nm [17] and the σ at this T_x was $0.375 \pm 0.01/nm^2$, the value of $\tilde{\sigma}^*$ at which the slope change occurred was 3.8 ± 0.1. At this $\tilde{\sigma}*$, the tethered PS chains start to get squeezed by neighbors and lateral repulsion builds up to affect the PEO block crystal growth in solution. The second PEO-*b*-PS sample possessed a different M_n^{PS} and was in amyl acetate. Note that amyl acetate is a very good solvent, and the mixed solvent is close to the θ condition for the PS blocks [17]. At $T_x^* = 28.3$ °C where the slope change took place, the value of $\tilde{\sigma}^*$ was again 3.8 ± 0.1.

If one follows the relationship of $d_L^{PEO} \propto 1/\Delta T$, the d_L^{PEO} increases should follow the dashed lines in Fig. 3(a). The only slightly increased d_L^{PEO} at temperatures above $T_x^* = 27.2$ °C and 28.3 °C destroyed this relationship. This is due to the additional repulsion caused by the squeezed and frustrated PS chains fighting to return to their most probable conformations which requires a larger coverage area. This repulsive force hampers the formation of thicker crystals and favors the growth of thinner crystals. In both cases, the slight increase of the d_L^{PEO} above the T_x^* is expected to result from the extra entropic surface free energy created by the repulsion which joins the nucleation barrier of the PEO block crystal growth at $T_x > T_x^*$.

In the case of the two PLLA-*b*-PS diblock copolymers (M_n^{PLLA} of 27.3 k and 56.8 k g/mol with M_n^{PS} of 6.0 k and 9.2 k g/mol, respectively) in amyl acetate, we also observed that changes in the slopes in the two plots of $(d_L^{PLLA})^{-1}$ with respect to T_x occurred at $T_x^* = 79.5$ °C and 74.3 °C (Fig. 4). Although the σ and/or the solvent type were different compared with those in the PEO-*b*-PS cases (about several times to an order of magnitude difference) and the values of R_g^{PS} of the $M_n^{PS} = 6.0$ k and 9.2 k g/mol in amyl acetate were 2.9 and 4.2 nm at 70 °C, respectively [17], both calculated values of $\tilde{\sigma}^*$ were 3.7 ± 0.1. In Fig. 4, we also include a linear relationship between $(d_L^{PLLA})^{-1}$ and T_x for a PLLA homopolymer crystallized at the same conditions. This indicates for the homopolymer, the relationship of $d_L^{PLLA} \propto 1/\Delta T$ does hold. It is interesting that the slope of this linear relationship is close to those for the PLLA-*b*-PS copolymers when $T_x < T_x^*$, revealing that below T_x^*, the growth of the PLLA blocks are not significantly affected by the PS blocks.

The results reported in this study have further implications for Fig. 1, which was originally a general representation of tethered chain molecules on a substrate. When the $\tilde{\sigma}$ of the PS blocks is lower than $\tilde{\sigma}^*$ at $T_x < T_x^*$,

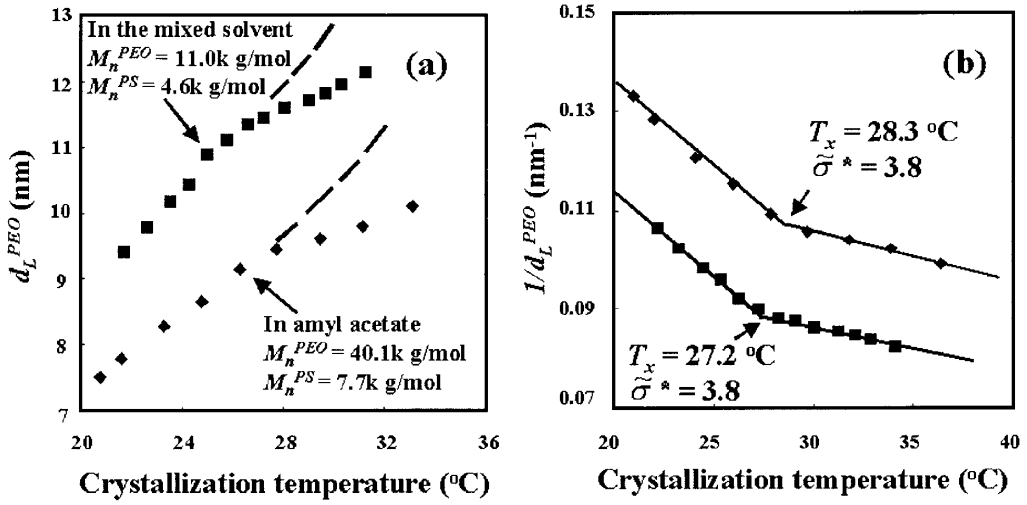

FIG. 3. Relationships of (a) the d_L^{PEO} values for two PEO-*b*-PS diblock copolymers with respect to T_x, and (b) the $(d_L^{PEO})^{-1}$ with respect to T_x in a close to θ solvent (chlorobenzene/octane) and a very good solvent (amyl acetate) for the PS blocks. At $Tx^* = 27.2$ °C and 28.3 °C, both the reduced tethering densities $\tilde{\sigma}^*$ are 3.8.

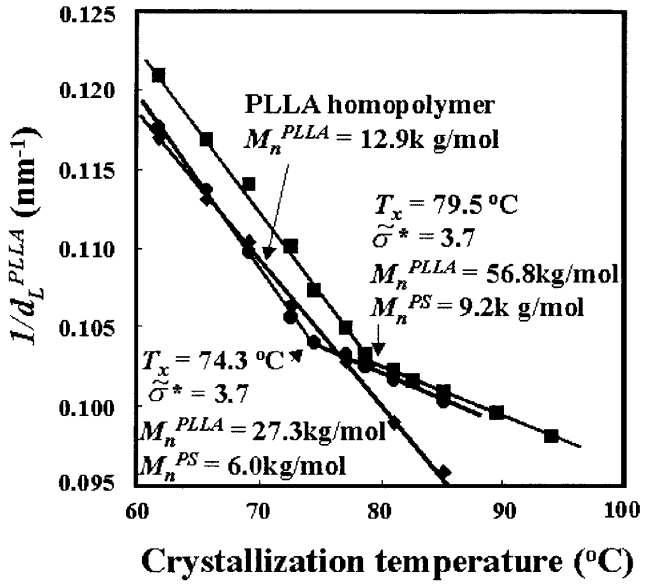

FIG. 4. Relationship between $(d_L^{\mathrm{PLLA}})^{-1}$ and T_x for the two PLLA-*b*-PS diblock copolymers with different MWs in a good solvent (amyl acetate) can be seen. At $Tx^* = 79.5\,^{\circ}\mathrm{C}$ and $74.3\,^{\circ}\mathrm{C}$, both of the reduced tethering densities $\tilde{\sigma}^*$ are 3.7. The $(d_L^{\mathrm{PLLA}})^{-1}$ versus T_x relationship for a homo-PLLA in the same solvent is also included.

the crystal growth in this T_x regime is kinetically controlled [18]. In the T_x regime where $T_x > T_x^*$, the crystalline blocks favor the growth of thicker crystals, which lowers the free energy by removing folds, but thicker crystals are disfavored by the amorphous blocks, which would have to stretch to accommodate them. This tradeoff of the free energy leads to an understanding that at each $T_x > \mathrm{T}_x^*$ in this T_x regime is "thermodynamically" controlled [18]. Note that the thickness still slightly increased with T_x as shown in Figs. 3 and 4, reflecting that at the T_x^* point the interaction between the amorphous PS blocks becomes so significant as to influence the d_L^{PEO} or d_L^{PLLA} within the broad crossover regime.

Quantitatively, the slope in the relationship between $(d_L)^{-1}$ versus T_x is equal to $\Delta H/(2T_d\gamma_e)$ (where ΔH is the heat of dissolution and γ_e is the folded surface free energy). The similar slopes of the $(d_L^{\mathrm{PLLA}})^{-1}$ versus T_x in these three cases thus imply that the values of γ_e for the homo-PLLA and two PLLA-*b*-PS crystals were similar below T_x^*. Compared with the slopes above T_x^*, the value of γ_e increases by a factor of 2.3. Similarly in the PEO-*b*-PS cases, the value of γ_e could be estimated to have changed by a factor of 2.5.

Based on the results of PEO and PLLA in four diblock copolymer systems, we conclude that the tethered PS chains do not become compressed in solution until $\tilde{\sigma}^*$ reaches ~3.7–3.8. As expected, MWs of the blocks and types of solvent used affect the T_x^* at which the tethered chains influence the crystal core thickness. However, the value of $\tilde{\sigma}^*$ should be MWand solvent independent, and is most likely universal for tethered chains.

This work was supported by the NSF (DMR-0203994).

*To whom correspondence should be addressed.
Email address: scheng@uakron.edu

[1] S. T. Milner, Science **251**, 905 (1991).
[2] A. Halperin, M. Tirrell, and T. P. Lodge, Adv. Polym. Sci. **100**, 31 (1992).
[3] B. Zhao and W. J. Brittan, Prog. Polym. Sci. **25**, 677 (2000).
[4] P. Mansky, Y. Liu, E. Huang, T. P. Russel, and C. J. Hawker, Science **275**, 1458 (1997).
[5] Y. Ito, Y. Ochiai, Y. S. Park, and Y. Imanishi, J. Am. Chem. Soc. **119**, 1619 (1997).
[6] H. J. Taunton *et al.*, Nature (London) **332**, 712 (1988).
[7] M. S. Kent, Macromol. Rapid Commun. **21**, 243 (2000).
[8] M. Adamuti-Trache, W. E. McMullen, and J. F. Douglas, J. Chem. Phys. **105**, 4798 (1996).
[9] M. A. Carignano and I. Szleifer, Macromolecules **28**, 3197 (1995).
[10] S. T. Milner, T. A. Witten, and M. E. Cates, Macromolecules **21**, 2610 (1988); **22**, 853 (1989).
[11] M. Murat and G. S. Grest, Macromolecules **22**, 4054 (1989); P.-Y. Lai and K. Binder, J. Chem. Phys. **95**, 9288 (1991); G. S. Grest and M. Murat, Macromolecules **26**, 3108 (1993).
[12] S. Alexander, J. Phys. (Paris) **39**, 983 (1977); P. G. de Gennes, Macromolecules **13**, 1069 (1980).
[13] T. Wu, K. Efimenko, and J. Genzer, J. Am. Chem. Soc. **124**, 9394 (2002).
[14] B. Lotz and A. J. Kovacs, Kolloid Z. Z. Polym. **209**, 97 (1966); B. Lotz, A. J. Kovacs, G. A. Bassett, and A. Keller, Kolloid Z. Z. Polym. **209**, 115 (1966).
[15] J. C. Wittmann and B. Lotz, Makromol. Chem. Rapid Commun. **3**, 733 (1982); J. C. Wittmann and B. Lotz, J. Polym. Sci. Polym. Phys. Ed. **23**, 205 (1985).
[16] Our differential scanning calorimetry measurements on the single crystals showed a normalized heat of fusion of 8.23 kJ/mol. Compared with the equilibrium heat of fusion of PEO crystals (8.66 kJ/mol), the crystallinity can be calculated to be 95%.
[17] The second Virial coefficient data of a series of monodispersed PS (M_n^{PS} = 4.6, 6.0, and 7.7 k and 9.2 k g/mol) in the mixed (chrolobenzene/octane) solvent and amyl acetate were measured at different temperatures in one of the co-author's laboratory (CW). The values of RgPS for the PS samples were estimated from the hydrodynamic radius in these solutions. For PS chains the mixed solvent is slightly better than the θ condition, while amyl acetate is a very good solvent for PS chains which is about 6 times better than the mixed solvent.
[18] E. A. DiMarzio, C. M. Guttman, and J. D. Hoffman, Macromolecules **13**, 1194 (1980).